

ual, B. Birren, E. D. Green, S. Klapholz, R. M. Myers, J. Roskams, Eds. (Cold Spring Harbor Laboratory Press, Cold Spring Harbor, NY, 1997), vol. 1, p. 301.

2. R. A. Gibbs, *Nature Genet.* **11**, 121 (1995); S. Ghosh *et al.*, *Genome Res.* **7**, 165 (1997).

3. For formation of the heaters, a 2- μm layer of *p*-xylylene was deposited as a moisture barrier and a reactive ion-hydrofluoric acid etch was used to form connections with the diodes. A 3.3- μm layer of Microposit 1400-37 photoresist was patterned to define the dual-meandering-line heaters (area 500 μm by 500 μm , line thickness 5 μm), and 50 nm of chromium was evaporated over the resist, followed by 400 nm of gold. Liftoff of the resist left the heaters on the surface. The heaters were then covered with a second, insulating layer of *p*-xylylene (2 μm thick).

4. For the electrodes, 20 nm of titanium and 30 nm of platinum were deposited on top of the second *p*-xylylene layer, using the same liftoff procedure as for the heaters.

5. Channels were prepared on 500- μm -thick glass wafers (Dow Corning 7740) using standard aqueous-based etch procedures, as described (7). Al (1000 nm) was then evaporated and patterned using photoresist AZP4620 (Hoechst Celanese). The wafer was dipped in a solution of heptadecafluoro-1,1,2,2-hydrodecyl dimethylchlorosilane to form hydrophobic regions on the surface, and the aluminum was then removed. Holes through the glass substrate at the ends of the fluid channels were drilled by applying 37 V to a metal point touching the glass surface in a 50 weight % sodium hydroxide solution. For assembly, the glass channel was placed on top of the silicon substrate, and optical adhesive (SK-9 Lens Bond; Sumers Laboratories, Fort Washington, PA) was applied to the edge of the channel and allowed to wick between the glass and silicon substrate. The adhesive did not enter the channel area and was cured under an ultraviolet lamp for 24 hours.

6. Raised polymer walls were fashioned around the buffer ports to prevent excess buffer from contacting the surface electronics. Monomer acrylamide electrophoresis gel material [10% acrylamide, 0.3% bis(acrylamide), 89 mM tris-HCl, 89 mM borate, 10 mM EDTA, 0.001% *N,N,N',N'*-tetramethylethylenediamine (TEMED), and 0.01% ammonium persulfate] was allowed to wick into the two channels and polymerize for 30 min. In some cases, a hydrophobic patch at the crossed channels was used to aid in the formation of flat gel interfaces. The gel present in two of the four channels of the intersection serves to restrict the motion of the sample and to ensure that the DNA remains at the running gel interface.

7. M. A. Burns *et al.*, *Proc. Natl. Acad. Sci. U.S.A.* **93**, 5556 (1996).

8. G. T. Walker *et al.*, *Nucleic Acids Res.* **20**, 1691 (1992). The enzyme solution contained 100 mM sodium chloride, 70 mM potassium phosphate, 20 mM tris (pH 7.6), 10 mM magnesium acetate, 2 mM dithiothreitol, Bst polymerase (0.5 U/ μl), and Bso B1 endonuclease (3.2 U/ μl per 25 μl). The DNA solution contained 2.8 mM 2'-deoxycytosine 5'-O-(1-thiotriphosphate) (dCTP- α -S), 0.4 mM each deoxynucleoside 5'-triphosphate (dATP, dGTP, dTTP), 1 μM primers, 0.1 μM bumpers, and target DNA (0.04 ng/ μl). The entire channel was rinsed with acetone, isopropyl alcohol, and bovine serum albumin (BSA) before each use. The target *Mycobacterium tuberculosis* DNA is 106 bp long and is the same as described in C. A. Spargo *et al.*, *Mol. Cell. Probes* **10**, 247 (1996). The amplified product was cloned into pGEM vector (pB959G) and sequenced for confirmation.

9. SDA does not work in the presence of intercalating dyes such as SYBR Green. For our integrated restriction digest runs, a separate dye injection step was not necessary; the dye was included in the DNA sample solution. Buffer was kept on the gel during reaction to prevent drying. The buffer was removed before the sample was loaded onto the gel.

10. Sample was removed after injection and replaced with buffer; runs were also performed without this step, but removing the sample led to more uniform and sharp peaks. Platinum electrodes placed in the buffer wells were used for both the injection and running of the sample.

11. A lock-in amplifier and data acquisition program were used to pulse a blue LED with accompanying low-pass filter at 288 Hz and to record the output of the microfabricated diode detector.

12. Diode detection limits for this system were obtained using dilute solutions of 4.0-kb plasmid DNA with intercalating dye. In a 50 μm by 500 μm channel over a 10 μm by 500 μm detector, DNA solutions at concentrations of 10 ng/ μl were readily detected.

13. S. N. Brahmasandra, B. N. Johnson, J. R. Webster, data not shown.

14. D. J. Harrison, A. Manz, Z. Fan, H. Ludi, H. M. Widmer, *Science* **261**, 895 (1993); J. M. Measros, G. Luo, J. Roeraade, A. G. Ewing, *Anal. Chem.* **65**, 3313 (1993); C. S. Effenhouser, A. Paulus, A. Manz, H. M. Widmer, *ibid.* **66**, 2949 (1994); S. C. Jacobson, L. B. Koutny, R. Hergenroder, A. W. Moore, J. M. Ramsey, *ibid.*, p. 3472; A. T. Woolley and R. A. Mathies, *Proc. Natl. Acad. Sci. U.S.A.* **91**, 11348 (1994); *Anal. Chem.* **67**, 3676 (1995); R. M. McCormick, R. J. Nelson, M. G. Alonso-amigo, D. J. Benvegno, H. H. Hooper, *ibid.* **69**, 2626 (1997); C. S. Effenhouser, F. J. M. Bruin, A. Paulus, M. Ehart, *ibid.*, p. 3451; P. C. Simpson *et al.*, *Proc. Natl. Acad. Sci. U.S.A.* **95**, 2256 (1998).

15. S. N. Brahmasandra, B. N. Johnson, J. R. Webster, data not shown.

16. K. Handique, B. P. Gogoi, D. T. Burke, C. H. Mas-trangelo, M. A. Burns, *SPIE Proc.* **3224**, 185 (1997).

17. B. N. Johnson, D. Jones, V. Namasivayam, M. A. Burns, data not shown.

18. When the reaction chamber is at 52°C, a thermocouple at the top surface of the glass (500 μm above) measures ~48°C. Therefore, the vertical temperature difference in the 50- μm -high channel is on the order of 0.5°C. A finite-difference solution of the heat-transfer equations for the system, using a constant-temperature boundary condition at the heater and a natural convection heat-transfer coefficient at the top, gives a similar result (T. S. Sammarco and M. A. Burns, data not shown).

19. Nanoliter reactions may be affected by evaporation and surface adsorption. Evaporation was reduced in our design by having only a few small openings from the device to the outside. Surface adsorption was reduced

by pretreatment of the microfluidic channels with a dilute protein solution (BSA); other researchers have solved the adsorption problem in different ways [for example, M. A. Shoffner, J. Cheng, G. E. Hivchik, L. J. Kricka, P. Wilding, *Nucleic Acids Res.* **24**, 375 (1996)].

20. D. T. Burke, M. A. Burns, C. H. Mastrangelo, *Genome Res.* **7**, 189 (1997).

21. M. V. Olson, *Science* **270**, 394 (1995); L. Rowen, G. Mahairas, L. Hood, *ibid.* **278**, 605 (1997); P. Green, *Genome Res.* **7**, 410 (1997).

22. A. T. Woolley *et al.*, *Anal. Chem.* **68**, 4081 (1996); A. G. Hadd, D. E. Raymond, J. W. Halliwell, S. C. Jacobson, J. M. Ramsey, *ibid.* **69**, 3407 (1997); A. T. Woolley, K. Lao, A. N. Glazer, R. A. Mathies, *ibid.* **70**, 684 (1998).

23. M. S. Chee *et al.*, *Science* **274**, 610 (1996); D. G. Wang *et al.*, *ibid.* **280**, 1077 (1998); R. G. Sosnowski, E. Tu, W. F. Butler, J. P. O'Connell, M. J. Heller, *Proc. Natl. Acad. Sci. U.S.A.* **94**, 1119 (1997); H. F. Arlinghaus, M. N. Kwoka, K. B. Jacobson, *Anal. Chem.* **69**, 3747 (1997).

24. As an example of the cost of these devices, a slightly more compact version of the current design would yield about 30 devices per wafer. The costs for 25 silicon and glass substrates are about \$600 and \$200, respectively. The lithography (\$500), ion implants and oxidation (\$100), high-pass optical filter (\$800), passivation layer (\$200), and depositions (\$500), along with laboratory fees (\$1700) to process 25 wafers, would therefore be \$3800, yielding a total device cost of just over \$6 per device. An optimized design combined with a larger batch run could easily bring the cost down by at least an order of magnitude.

25. Supported by the National Center for Human Genome Research, NIH (R01-HG01044, R01-HG01406). We thank Becton Dickinson for its support during M.A.B.'s sabbatical and L. Lawton for her help in performing SDA. Computer files for generating the fabrication masks and for the computer instrumentation controls are available on request.

28 May 1998; accepted 2 September 1998

Phosphorylation and Activation of 13S Condensin by Cdc2 in Vitro

Keiji Kimura, Michiko Hirano, Ryuji Kobayashi, Tatsuya Hirano*

13S condensin is a multisubunit protein complex essential for mitotic chromosome condensation in *Xenopus* egg extracts. Purified 13S condensin introduces positive supercoils into DNA in the presence of topoisomerase I and adenosine triphosphate in vitro. The supercoiling activity of 13S condensin was regulated by mitosis-specific phosphorylation. Immunodepletion, in vitro phosphorylation, and peptide-mapping experiments indicated that Cdc2 is likely to be the kinase that phosphorylates and activates 13S condensin. Multiple Cdc2 phosphorylation sites are clustered in the carboxyl-terminal domain of the XCAP-D2 (*Xenopus* chromosome-associated polypeptide D2) subunit. These results suggest that phosphorylation of 13S condensin by Cdc2 may trigger mitotic chromosome condensation in vitro.

Chromosome condensation is a fundamental cellular process that ensures the faithful segregation of genetic information during mitosis and meiosis. Activation of the protein kinase Cdc2 triggers a series of downstream

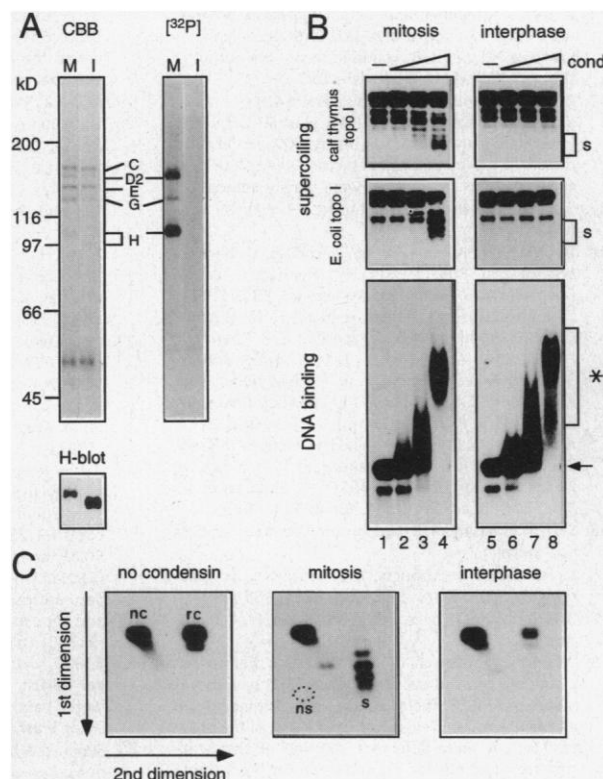
mitotic events including chromosome condensation, but the underlying molecular mechanisms are poorly understood (1, 2). 13S condensin, a five-subunit protein complex purified from *Xenopus* egg extracts, is an essential regulator of mitotic chromosome condensation (3, 4). The two core subunits of 13S condensin, XCAP-C and XCAP-E, belong to the SMC (structural maintenance of

Cold Spring Harbor Laboratory, Post Office Box 100, 1 Bungtown Road, Cold Spring Harbor, NY 11724, USA.

*To whom correspondence should be addressed.

REPORTS

Fig. 1. Mitosis-specific and phosphorylation-dependent supercoiling activity of 13S condensin. **(A)** Characterization of 13S condensin purified from a mitotic (M) or an interphase (I) extract (8). CBB, Coomassie stain; [³²P], autoradiography of condensin subunits purified from ³²P-labeled extracts; C, XCAP-C; D2, XCAP-D2; E, XCAP-E; G, XCAP-G; H, XCAP-H; H-blot, immunoblot with anti-XCAP-H. **(B)** Supercoiling and DNA binding activities of the mitotic (lanes 2 to 4) or interphase (lanes 6 to 8) form of 13S condensin (cond.). Calf thymus (top) or *E. coli* (middle) topoisomerase I was supplemented into the supercoiling reactions but was omitted in the DNA binding assay (bottom) (7). DNA was purified (top and middle) or unpurified (bottom), electrophoresed on a 0.7% agarose gel, and visualized by Southern blotting (9). The molar ratios of 13S condensin to DNA in the reaction mixtures were ~9:1 (lanes 2 and 6), ~18:1 (lanes 3 and 7), or ~36:1 (lanes 4 and 8). Lanes 1 and 5, no protein; s, positively supercoiled DNA; arrow, free DNA; asterisk, DNA bound to 13S condensin. **(C)** Two-dimensional gel electrophoresis. Substrate DNA (a mixture of nicked circular and relaxed circular DNA) was subjected to the supercoiling assay with *E. coli* topoisomerase I, fractionated on a two-dimensional agarose gel, and visualized by Southern blotting (9). Left, no condensin; center, mitotic 13S condensin; right, interphase 13S condensin. The molar ratio of protein to DNA was ~36:1. Abbreviations: nc, nicked circular DNA; rc, relaxed circular DNA; s, positively supercoiled DNA; ns, expected position where negatively supercoiled DNA migrates.



chromosomes) family of chromosomal adenosine triphosphatases (ATPases) (2, 5). The remaining three subunits, XCAP-D2, XCAP-G, and XCAP-H, may have regulatory roles in condensin function (4). Genetic studies in yeasts, *Drosophila*, and *Caenorhabditis elegans* show that (at least some of) the condensin subunits are essential for chromosome condensation and segregation in vivo (6). When purified from mitotic extracts, 13S condensin has a DNA-stimulated ATPase activity and can introduce positive supercoils into relaxed circular DNA in the presence of ATP and topoisomerase I. This activity may contribute to chromosome condensation during mitosis (7).

To test whether the positive supercoiling activity of 13S condensin is regulated during the cell cycle, we purified 13S condensin from mitotic or interphase extracts of *Xenopus* eggs by immunoaffinity column chromatography (8). The subunit compositions of the two forms were indistinguishable, although three of the five subunits (XCAP-D2, XCAP-G, and XCAP-H) were phosphorylated in a mitosis-specific manner (Fig. 1A) (4). Because of this modification, the electrophoretic mobility of the mitotic form of XCAP-H was decreased (Fig. 1A). When this mitotic form of 13S condensin was incubated with a relaxed circular DNA in the presence of ATP and topoisomerase I (purified from calf thymus or *Escherichia coli*), the DNA was converted into a ladder of supercoiled forms in a dose-dependent manner (Fig. 1B) (9). In contrast, the supercoiling activity was barely detectable in the interphase form of 13S condensin, although it exhibited a DNA binding activity comparable to that of the mitotic form of 13S condensin (Fig. 1B, bottom). Two-dimensional gel electrophoresis confirmed that the mitotic condensin induced positive supercoiling (Fig. 1C). Changes in the average linking number of the substrate DNA were measured to be +3.3 with the mitotic form and +0.1 with the interphase form under this condition (9). The supercoiling activity was highly reproducible between different preparations. Treatment of the mitotic condensin with λ protein phosphatase (λ -PPase) resulted in a decrease in supercoiling activity accompanied by dephosphorylation of the three subunits (10), which suggested that the activity is regulated by mitosis-specific phosphorylation.

In an attempt to identify the kinase or kinases that activate the supercoiling activity of 13S condensin, we immunodepleted Cdc2 from a mitotic extract (11). The efficiency of immunodepletion was estimated to be >95% by both immunoblotting and measurement of histone H1 kinase activity (Fig. 2A). Depletion of Cdc2 resulted in reduced phosphorylation of the condensin subunits and loss of the condensation activity of the extract. In a

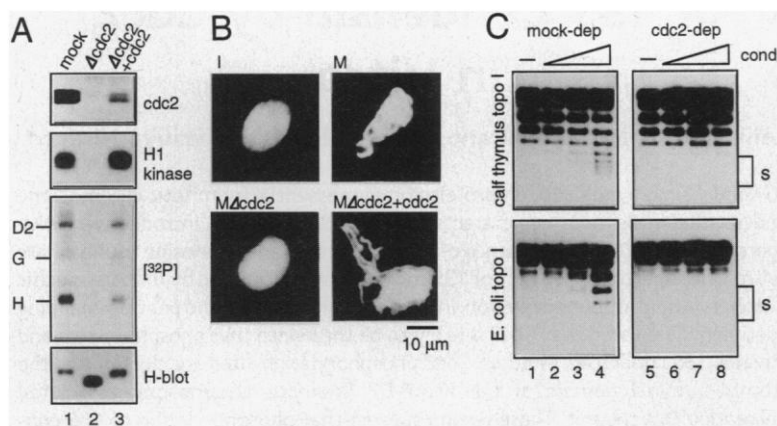


Fig. 2. Control of supercoiling activity of 13S condensin by Cdc2. **(A)** Effects of Cdc2 depletion. Mitotic extracts were immunodepleted with control immunoglobulin G (lane 1) or anti-Cdc2 (lanes 2 and 3) (11), and Cdc2-cyclin B purified from a *Xenopus* egg extracts (13) was added back to one portion of the depleted extract (lane 3). Amounts of Cdc2 protein (cdc2) and histone H1 kinase activity in the extracts were measured. Phosphorylation of condensin subunits was analyzed by immunoprecipitation from ³²P-labeled extracts ([³²P]) or by immunoblotting with anti-XCAP-H (H-blot). **(B)** Condensation assay. *Xenopus* sperm chromatin was mixed with an interphase (I), mock-depleted mitotic (M), Cdc2-depleted mitotic (M Δ cdc2), or Cdc2-reconstituted (M Δ cdc2+cdc2) extract. After 3 hours at 22°C, chromatin was fixed and stained with 4',6'-diamidino-2-phenylindole (DAPI) (12). **(C)** Supercoiling activity of 13S condensin purified from the mock-depleted (lanes 2 to 4) or Cdc2-depleted (lanes 6 to 8) extracts. Lanes 1 and 5, no protein. The molar ratios of protein to DNA were the same as in Fig. 1B.

REPORTS

control mitotic extract, sperm chromatin underwent a series of structural changes and was eventually transformed into a cluster of mitotic chromosomes (Fig. 2B) (12). In contrast, the chromatin was converted into a round structure in the Cdc2-depleted extract that was indistinguishable from the chromatin assembled in an interphase extract (Fig. 2B). When purified Cdc2–cyclin B (13) was added back into the depleted extract, the condensation activity was restored, accompanied by phosphorylation of the condensin subunits (Fig. 2A). The supercoiling activity of 13S condensin purified from the Cdc2-depleted extract was reduced relative to that from the control extract (Fig. 2C).

These results suggest that 13S condensin

is phosphorylated and activated either by Cdc2 itself or by kinases activated by Cdc2. Several consensus sites for phosphorylation by Cdc2 (14) exist in the sequences of XCAP-D2 (15, 16) and XCAP-H (4), and we tested whether purified Cdc2 phosphorylated these subunits in vitro. A purified Cdc2–cyclin B fraction phosphorylated the XCAP-D2 and XCAP-H subunits of 13S condensin isolated from an interphase extract (Fig. 3A) (17). This treatment converted the interphase 13S condensin into an active form that supported positive supercoiling of DNA (Fig. 3B). Two-dimensional tryptic phosphopeptide mapping (18) revealed three major peptides of XCAP-D2 phosphorylated by Cdc2–cyclin B that aligned with those labeled in

mitotic extracts (Fig. 3C), suggesting that Cdc2 itself may phosphorylate XCAP-D2 in mitotic extracts. The maps of XCAP-H were more complex: At least 10 spots were detected in mitotic extracts, and five of them migrated with peptides phosphorylated by Cdc2–cyclin B. Thus, additional kinases are apparently required for full phosphorylation of XCAP-H. Nevertheless, after phosphorylation by Cdc2–cyclin B, the specific activity of 13S condensin from interphase extracts was comparable to that of 13S condensin purified from mitotic extracts.

To test whether Cdc2 consensus sites in the COOH-terminal region of XCAP-D2 are phosphorylated by Cdc2, we synthesized three phosphopeptides, each of which contained a single phosphothreonine, and prepared phospho-specific antibodies (19). The peptides were DP1 (EDDFQphosphoT¹³¹⁴PKPPA), DP2 (LSEAEphosphoT¹³⁴⁸PKNPT), and DP3 (TPKNPphosphoT¹³⁵³PIRRP) (16). Affinity-purified anti-DP1 recognized the mitotic form, but not the interphase form, of XCAP-D2, nor did it recognize the mitotic form that had been treated with λ -PPase (Fig. 4A). Antibody binding was blocked by the DP1 peptide, but not with an unphosphorylated peptide of the same sequence (DU1) or the other two phosphopeptides (Fig. 4B). Thus, anti-DP1 appears to recognize mitosis-specific phosphothreonine Thr¹³¹⁴ of XCAP-D2. Similarly, anti-DP2 and anti-DP3 recognized mitosis-specific phosphothreonines Thr¹³⁴⁸ and Thr¹³⁵³, respectively (Fig. 4, A and B). Immunodepletion of Cdc2 from a mitotic extract resulted in a loss of the three phosphoepitopes from XCAP-D2, and incubation of the interphase form of XCAP-D2 with purified Cdc2–cyclin B led to phosphorylation of these epitopes (Fig. 4A). Thus, the three sites clustered in the COOH-terminal domain are likely to be the physiological and direct targets of Cdc2. XCAP-D2 also acquired an MPM-2 epitope in a mitosis-specific and Cdc2-dependent manner [MPM-2 is a monoclonal antibody that recognizes mitosis-specific phosphoepitopes] (12, 20).

These results provide evidence for a direct functional link between the master mitotic kinase, Cdc2, and the key machinery of chromosome condensation. The supercoiling activity of 13S condensin may be a physiologically relevant activity that is essential for mitotic chromosome condensation.

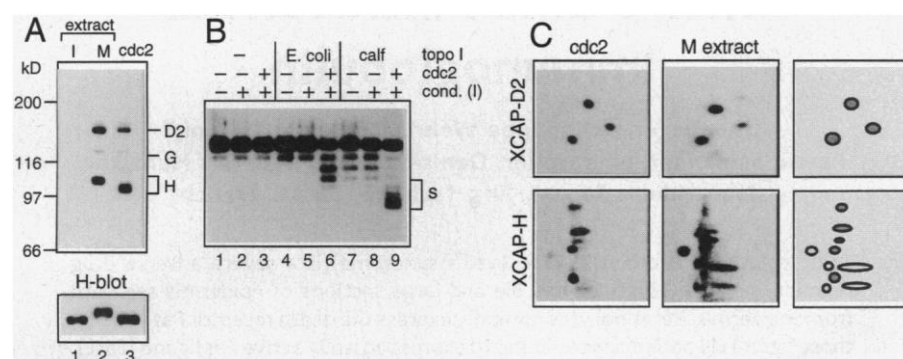


Fig. 3. Phosphorylation and activation of 13S condensin by Cdc2. (A) Phosphorylation of XCAP-D2 and XCAP-H by Cdc2–cyclin B in vitro. 13S condensin was immunoprecipitated from ³²P-labeled interphase (lane 1) or mitotic (lane 2) extract (8). Alternatively, 13S condensin was purified from an interphase extract and then incubated with purified Cdc2–cyclin B in the presence of [γ -³²P]ATP (lane 3) (17). The labeled proteins were analyzed by autoradiography (top) or by immunoblotting with anti-XCAP-H (bottom). (B) Supercoiling assay of 13S condensin phosphorylated by Cdc2–cyclin B. Interphase 13S condensin was phosphorylated by Cdc2–cyclin B (lanes 3, 6, and 9) or treated with buffer alone (lanes 2, 5, and 8) (17). Supercoiling assay was done in the presence of no topoisomerase (lanes 1 to 3) or type I topoisomerases from *E. coli* (lanes 4 to 6) or calf thymus (lanes 7 to 9). (C) Phosphopeptide mapping of XCAP-D2 (upper panels) and XCAP-H (lower panels) labeled by purified Cdc2–cyclin B (left) or in mitotic extracts (center) as described in (A) (18). (Right) spots overlapping under the two conditions are indicated by filled circles, and those unique to mitotic extracts are indicated by open circles.

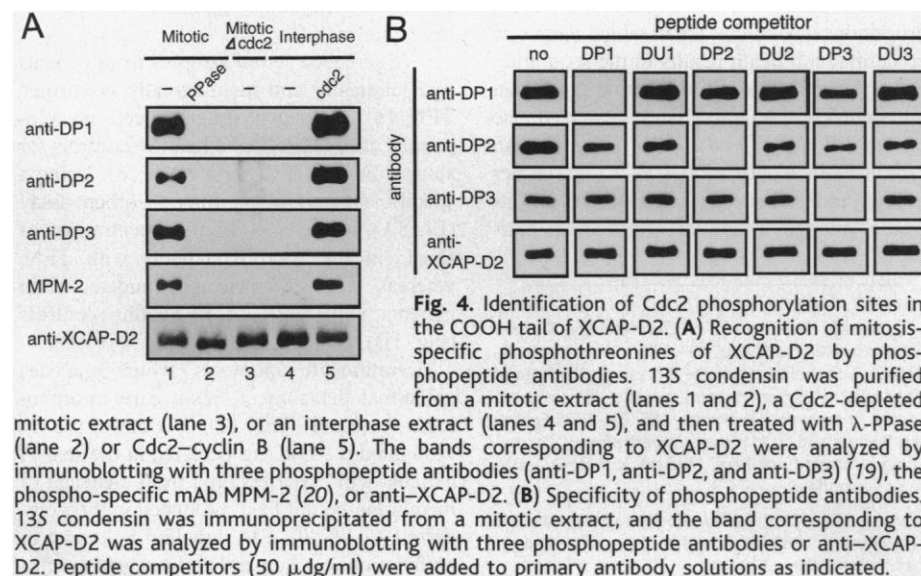


Fig. 4. Identification of Cdc2 phosphorylation sites in the COOH tail of XCAP-D2. (A) Recognition of mitosis-specific phosphothreonines of XCAP-D2 by phosphopeptide antibodies. 13S condensin was purified from a mitotic extract (lanes 1 and 2), a Cdc2-depleted mitotic extract (lane 3), or an interphase extract (lanes 4 and 5), and then treated with λ -PPase (lane 2) or Cdc2–cyclin B (lane 5). The bands corresponding to XCAP-D2 were analyzed by immunoblotting with three phosphopeptide antibodies (anti-DP1, anti-DP2, and anti-DP3) (19), the phospho-specific mAb MPM-2 (20), or anti-XCAP-D2. (B) Specificity of phosphopeptide antibodies. 13S condensin was immunoprecipitated from a mitotic extract, and the band corresponding to XCAP-D2 was analyzed by immunoblotting with three phosphopeptide antibodies or anti-XCAP-D2. Peptide competitors (50 μ g/ml) were added to primary antibody solutions as indicated.

References and Notes

1. A. Murray and T. Hunt, *The Cell Cycle: An Introduction* (Freeman, New York, 1993); P. Nurse, *Nature* **344**, 503 (1990).
2. D. Koshland and A. Strunnikov, *Annu. Rev. Cell Dev. Biol.* **12**, 305 (1996).
3. T. Hirano and T. J. Mitchison, *Cell* **79**, 449 (1994).
4. T. Hirano, R. Kobayashi, M. Hirano, *ibid.* **89**, 511 (1997).
5. T. Hirano, *Curr. Opin. Cell Biol.* **10**, 317 (1998); R. Jessberger, C. Frei, S. M. Gasser, *Curr. Opin. Genet. Dev.* **8**, 254 (1998).
6. Y. Saka *et al.*, *EMBO J.* **13**, 4938 (1994); A. V. Strun-

nikov, E. Hogan, D. Koshland, *Genes Dev.* **9**, 587 (1995); M. A. Bhat, A. V. Philp, D. M. Glover, H. J. Bellen, *Cell* **87**, 1103 (1996); J. D. Lieb, M. R. Albrecht, P.-T. Chuang, B. J. Meyer, *ibid.* **92**, 265 (1998).

7. K. Kimura and T. Hirano, *Cell* **90**, 625 (1997).

8. Immunoaffinity purification of 13S condensin was done as described (7); for more details, see *Science Online* (www.sciencemag.org). 13S condensin preparations from two different metaphase extracts [extracts from metaphase II-arrested eggs and extracts activated by cyclin BΔ90 (a nondegradable form of cyclin B)] had identical subunit compositions and supercoiling activities. We do not distinguish between the two preparations and refer to them as the mitotic form throughout this report. Similarly, 13S condensin purified from two different interphase extracts (extracts from eggs activated with the calcium ionophore A23187 and extracts activated in vitro by addition of CaCl₂) were indistinguishable. The cell cycle-specific extracts were prepared as described [A. W. Murray, *Methods Cell Biol.* **36**, 581 (1991); T. Hirano and T. J. Mitchison, *J. Cell Biol.* **115**, 1479 (1991)].

9. Supercoiling assay was done as described (7); for more details, see *Science Online* (www.sciencemag.org). Linking number is a parameter that describes the topological state of a closed circular DNA and corresponds to the number of times that the two chains of DNA twist around one another.

10. K. Kimura and T. Hirano, unpublished data.

11. H. Masuda and T. Shibata, *J. Cell Sci.* **109**, 165 (1996).

12. T. Hirano and T. J. Mitchison, *J. Cell Biol.* **120**, 601 (1993).

13. M. J. Solomon, T. Lee, M. W. Kirschner, *Mol. Biol. Cell* **3**, 13 (1992). For reconstitution, Cdc2 was added at 20 to 80% of the endogenous level.

14. E. A. Nigg, *Trends Cell Biol.* **3**, 296 (1993); J. K. Holmes and M. J. Solomon, *J. Biol. Chem.* **271**, 25240 (1996).

15. A mixture of 8S and 13S condensins was immunoprecipitated with anti-XCAP-E, and the XCAP-D2 subunit was gel-purified and processed for microsequencing as described (4). On the basis of two peptide sequences obtained (MEDDFQTPKPPASRK and ENPDYIMAK) (16), we cloned XCAP-D2 cDNA by the reverse transcription-polymerase chain reaction (RT-PCR), two rounds of library screening, and nested PCRs. The full-length cDNA was constructed from multiple overlapping cDNAs and sequenced. The cDNA predicted a 1364-amino acid polypeptide with a calculated molecular weight of 154 kD and a pI of 5.46 (GenBank accession number AF067969). A database search identified homologs of unknown functions from yeast (YLR272C), *C. elegans* (ALO21482), and human (D63880).

16. Abbreviations for the amino acid residues are as follows: A, Ala; C, Cys; D, Asp; E, Glu; F, Phe; G, Gly; H, His; I, Ile; K, Lys; L, Leu; M, Met; N, Asn; P, Pro; Q, Gln; R, Arg; S, Ser; T, Thr; V, Val; W, Trp; and Y, Tyr.

17. 13S condensin (~90 ng) purified from an interphase extract was incubated at 22°C for 30 min in 5 μl of buffer [10 mM Hepes-KCl (pH 7.7), 50 mM KCl, 2 mM MgCl₂, 0.1 mM CaCl₂, 1 mM MgATP, 5 mM EGTA, 1 mM dithiothreitol, and ovalbumin (1 mg/ml)] containing purified Cdc2-cyclin B (~0.1 ng) (13). A 3-μl aliquot was used in a 5-μl supercoiling reaction (9). Purified Cdc2-cyclin B alone displayed no supercoiling activity. Two other kinases were used as controls. Casein kinase II phosphorylated XCAP-D2 and XCAP-H, but none of the three Cdc2 consensus sites of XCAP-D2 were phosphorylated, as judged by cross-reactivity to the phosphopeptide antibodies (19). MAP kinase (Erk2) barely phosphorylated the condensin subunits. Neither kinase activated the supercoiling activity of 13S condensin.

18. G. L. Russo et al., *J. Biol. Chem.* **267**, 20317 (1992).

19. A synthetic peptide corresponding to the COOH-terminal sequences of XCAP-D2 (CNPTPIRRTARSRAK) was used to prepare an antibody that recognizes both the mitotic and interphase forms of XCAP-D2. To prepare phospho-specific antibodies, we synthesized three phosphopeptides and the corresponding unphosphorylated peptides. The sequences were as follows: DP1, CEDDFQphosphoTPKPPA; DU1, CEDDFQTPKPPA; DP2, CLSEAEphosphoTPKNPT; DU2, CLSEAETPKNPT; DP3,

CTPKNpphosphoTPIRRT; DU3, CTPKNPTPIRRT (16). A crude serum raised against the DPx (x = 1, 2, or 3) peptide was passed through an Affi-Gel 10 (Bio-Rad) column conjugated with DUx, and then its flowthrough fraction was loaded onto a second column conjugated with DPx. After extensive washing, phospho-specific antibody was eluted by low pH and used as an affinity-purified anti-DPx. Conjugation of the peptides to a carrier protein and affinity purification of specific antibodies were done as described [K. E. Sawin, T. J. Mitchison, L. G. Wordeman, *J. Cell Sci.* **102**, 303 (1992)].

20. F. M. Davis, T. Y. Tsao, S. K. Fowler, P. N. Rao, *Proc. Natl. Acad. Sci. U.S.A.* **80**, 2926 (1983); T. Hirano and

T. J. Mitchison, *J. Cell Biol.* **115**, 1479 (1991); S. Taagepera, P. N. Rao, F. H. Drake, G. J. Gorbsky, *Proc. Natl. Acad. Sci. U.S.A.* **90**, 8407 (1993).

21. We thank H. Masuda for anti-*Xenopus* Cdc2 antiserum, M. Solomon for the GST-cyclin B plasmid, J. Hemish for her help with the characterization of phosphopeptide antibodies, and J. Swedlow and A. Losada for their comments. Supported by NIH grant GM53926 and the Pew Scholars Program in the Biomedical Sciences (T.H.), NIH grant CA45508 (R.K.), and fellowships from the Leukemia Society of America and the Robertson Research Fund (K.K.).

26 March 1998; accepted 14 September 1998

Inhibition of Toxic Epidermal Necrolysis by Blockade of CD95 with Human Intravenous Immunoglobulin

Isabelle Viard, Philippe Wehrli,* Roberto Bullani,* Pascal Schneider, Nils Holler, Denis Salomon, Thomas Hunziker, Jean-Hilaire Saurat, Jürg Tschopp, Lars E. French†

Toxic epidermal necrolysis (TEN, Lyell's syndrome) is a severe adverse drug reaction in which keratinocytes die and large sections of epidermis separate from the dermis. Keratinocytes normally express the death receptor Fas (CD95); those from TEN patients were found to express lytically active Fas ligand (FasL). Antibodies present in pooled human intravenous immunoglobulins (IVIG) blocked Fas-mediated keratinocyte death in vitro. In a pilot study, 10 consecutive individuals with clinically and histologically confirmed TEN were treated with IVIG; disease progression was rapidly reversed and the outcome was favorable in all cases. Thus, Fas-FasL interactions are directly involved in the epidermal necrolysis of TEN, and IVIG may be an effective treatment.

Alterations in the control of apoptosis, a type of cell death, are involved in the pathogenesis of several human diseases (1, 2). Apoptosis can be triggered by interaction between a cell-surface death receptor such as Fas and its respective ligand (Fas ligand: FasL or CD95L).

TEN (or Lyell's syndrome) is a severe drug-induced skin disease in which apoptotic epidermal cell death results in the separation of large areas of skin at the dermo-epidermal junction (Fig. 1A), producing the appearance of scalded skin (3, 4). TEN occurs at an estimated incidence of 0.4 to 1.2 cases per million, most frequently as a result of sulfonamide, anticonvulsant, or nonsteroidal anti-

inflammatory drug use, and is associated with a mortality rate of about 30% (3, 5). There is no known effective treatment for TEN. Keratinocyte apoptosis is rare in the normal epidermis, but is abnormally increased during TEN (3, 4). The mechanisms responsible for enhanced keratinocyte apoptosis in TEN remain unclear (4).

We screened serum samples from patients with clinically and histologically confirmed TEN (6), extensive drug-induced maculopapular rash (MPR), and healthy controls for soluble FasL (sFasL) content (7, 8). Using a specific enzyme-linked immunosorbent assay (ELISA), we detected high concentrations of sFasL in the sera of patients with TEN, whereas sFasL was virtually undetected in patients with MPR or in healthy controls (Fig. 1B).

Keratinocyte apoptosis, which precedes epidermal detachment, is an early morphologic feature of TEN (4). Therefore, we investigated if the sFasL detected in the sera of patients with TEN resulted from cleavage of membrane-bound FasL produced in their epidermis (7, 9, 10). Fas signaling is known to be functional in human keratinocytes in vitro

I. Viard, P. Wehrli, R. Bullani, D. Salomon, J.-H. Saurat, L. E. French, Department of Dermatology, Geneva University Medical School, CH-1211 Geneva 4, Switzerland. P. Schneider, N. Holler, J. Tschopp, Institute of Biochemistry, University of Lausanne, BIL Research Center, Chemin des Boveresses 155, CH-1066 Epalinges, Switzerland. T. Hunziker, Department of Dermatology, University of Bern, Medical School, CH-3010 Bern, Switzerland.

*These authors contributed equally to this work.

†To whom correspondence should be addressed. E-mail: french@cmu.unige.ch